Supplement of Geosci. Model Dev., 17, 1387–1407, 2024
https://doi.org/10.5194/gmd-17-1387-2024-supplement

Geoscientific Model Development
Open Access
EGU

Supplement of

Numerical coupling of aerosol emissions, dry removal, and turbulent mixing in the E3SM Atmosphere Model version 1 (EAMv1) – Part 1: Dust budget analyses and the impacts of a revised coupling scheme

Hui Wan et al.

Correspondence to: Hui Wan (hui.wan@pnnl.gov)

1 Interstitial dust mass mixing ratios and tendencies in source-vicinity and remote regions

Figure 5 in the paper shows statistical distributions of instantaneous dust mass tendencies caused by various physical processes as well as the mass mixing ratios after those processes have been calculated and applied. There, the results are shown for dust source regions, i.e., grid columns in the box with solid outline in Fig. 3a that have instantaneous emission fluxes that fall into the middle portion of the histogram shown in Fig. 4. Figures S1 and S2 below show the corresponding results for the source-vicinity regions in the box with solid outline in Fig. 3a and the remote region indicated by the box with dashed outline in Fig. 3a, respectively.

2 Impact of the revised process coupling on various aerosol species in EAMv1

The revision of process coupling as described in Sect. 3.3 of the paper has been applied to not only dust but also the other aerosol species in the MAM4 parameterization package. Five out of the 7 aerosol species in MAM4, namely dust, sea salt, MOA, BC, and POA, have large portions (50% or more) of their sources coming from surface emissions. The other two species, sulfate and SOA, are predominantly or 100% produced in the atmosphere. Therefore, we expect the revised coupling to have discernable impacts on the first 5 aerosol species mentioned above but negligible direct impacts on sulfate and SOA.

In Table S1, we show the vertically integrated and annually averaged dry removal rates for regions with or without surface emissions as well as for the entire globe, for the 5 aerosol species with substantial surface sources. (The process rates shown here have included contributions from both interstitial and cloud-borne aerosols to facilitate a direct comparison with the diagnostics typically used by the MAM model developers.) The relative differences listed in the table reveal consistent results among the different species, namely dry removal becomes weaker in regions with surface emissions but stronger in regions without surface emissions. The global averages, which are dominated by the results in the source regions, show a general trend of weaker dry removal when the revised coupling is used.

It is worth noting that among those five aerosol species that have substantial surface emissions, dust and sea salt emissions introduce particles primarily to MAM4's coarse mode (where the mode's geometric mean diameter range is 1 μm $\leqslant D_p \leqslant$ 4 μm), while MOA, BC, and POA emissions add particles mostly to MAM4's primary carbon mode (10 nm $\leqslant D_p \leqslant$ 100 nm) and accumulation mode (53.5 nm $\leqslant D_p \leqslant$ 440 nm). Although there are various mechanisms for different aerosol species to mix and for aerosol particles to grow in the atmosphere, MOA, BC, and POA are predominantly found in aerosol particles of submicron diameters. Since smaller particles are less susceptible to dry removal, we expect to see smaller impacts of the revised coupling on the atmospheric load of MOA, BC, and POA than on dust and sea salt. This reasoning is confirmed by the 10-year mean zonally averaged mass mixing ratios shown in Fig. S3. The relative changes in zonal mean mixing ratio shown in the rightmost column in Fig. S3 further confirm the large impacts on dust and sea salt and the smaller impacts on the predominantly submicron species (MOA, BC, POA). As for sulfate, SOA, and precursor gases in EAMv1, the changes in zonal and annual mean mixing ratios are small and insignficant and hence not shown.

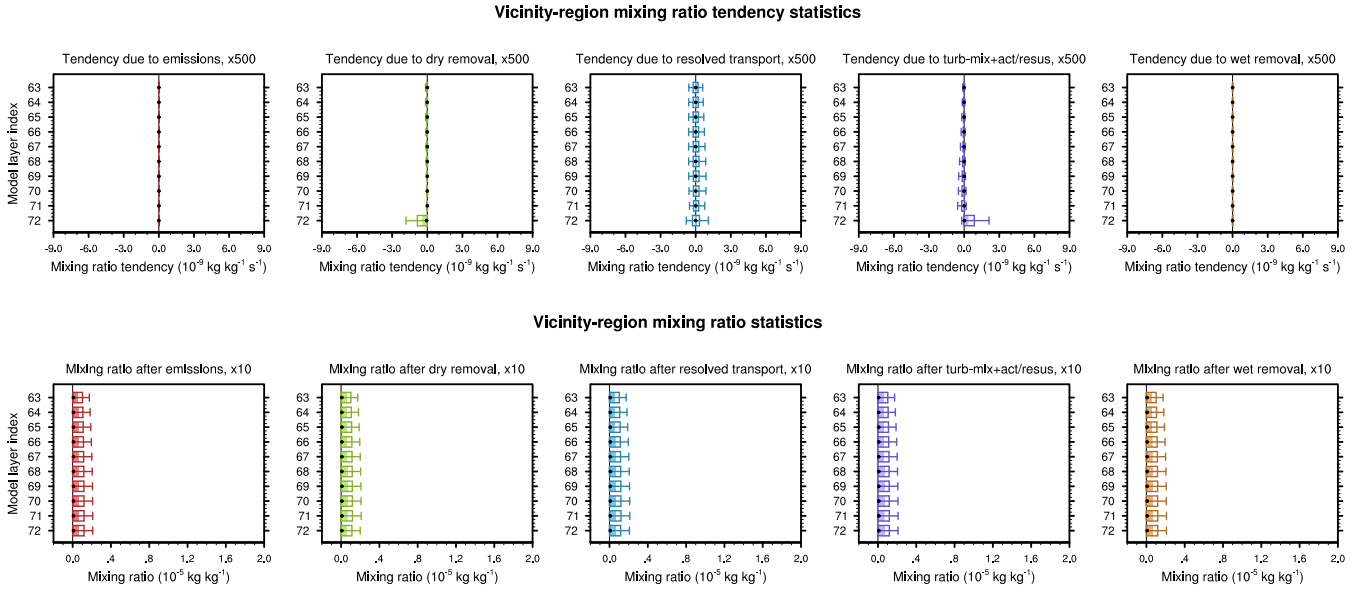

Figure S1. As in Fig. 5 of the paper but showing results in the source-vicinity regions indicated by the box with solid outline in Fig. 3a. The tendencies in the upper row and the mixing ratio in the lower row have been multiplied by 500 and 10, respectively, in order to be plotted with the same x axis ranges as in Fig. 5 of the paper.

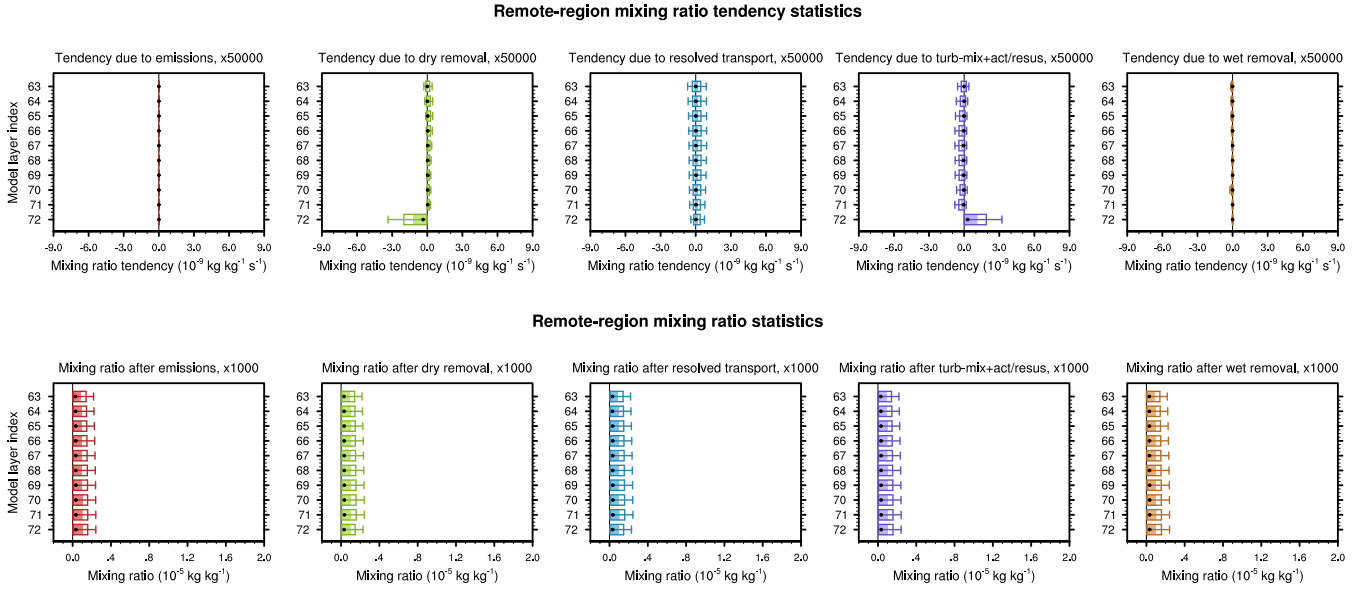

Figure S2. As in Fig. 5 of the paper but showing results in the remote region indicated by the box with dashed outline in Fig. 3a. The tendencies in the upper row and the mixing ratio in the lower row have been multiplied by 5×10^4 and 1000, respectively, in order to be plotted with the same x axis ranges as in Fig. 5 of the paper.

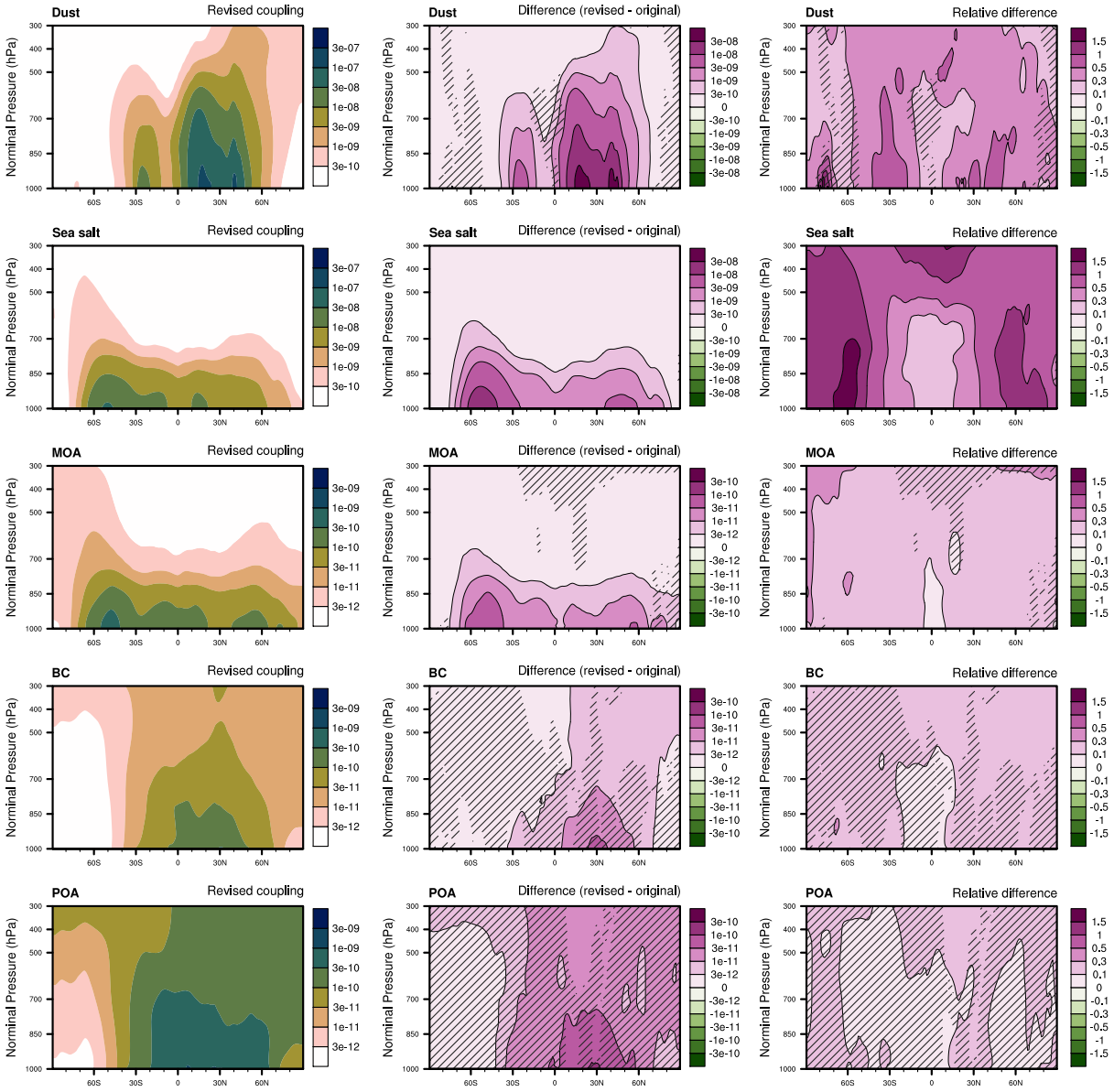

Figure S3. Comparison of the 10-year mean zonally averaged mass mixing ratio (unit: kg kg^{-1}) of various aerosol species simulated with EAMv1 using the original or revised process coupling and with the L72 vertical grid. The different rows correspond to the 5 aerosol species in MAM4 that have significant surface emissions. Left column shows the L72 simulation using the revised coupling scheme. Middle column shows the changes caused by the revision in process coupling. Right column shows the relative differences with respect to the original model. The hatched locations in the middle and right columns are where the differences between the two 10-member ensembles of one-year averages are statistically insignificant according to the Kolmogorov–Smirnov two-sample test at a significance level of 0.05.

Table S1. Similar to Table 1 in the paper but showing the impact of the revised process coupling on dry removal of aerosol species that have substantial surface emissions. Here, source region and non-source region refer to geographical locations with or without surface emissions of the corresponding aerosol species. Whether a grid column had emissions was determined separately for each simulation and for each year between 2000 and 2009 using the annual mean emission fluxes. The 1-year mean, vertically integrated dry removal rates were then integrated horizontally to give dry removal rates in the unit of Tg yr^{-1}. After that, the mean and standard deviation of the yearly values of spatial integrals were calculated. In the table, the standard deviation is shown in parentheses and expressed as the percentage of the corresponding 10-year mean. The relative differences of 10-year averages are shown as percentages without parentheses. (We note that the dry removal rates shown in this table have included contributions from both interstitial and cloud-borne aerosols to facilitate a direct comparison with the diagnostics typically used by the MAM model developers.)

	Source-region total			**Non-source-region total**			**Global total**		
	Original	Revised	Rel. diff.	Original	Revised	Rel. diff.	Original	Revised	Rel. diff.
Dust	-2704 ($\pm4\%$)	-1733 ($\pm4\%$)	-36%	-784 ($\pm5\%$)	-1408 ($\pm4\%$)	$+80\%$	-3488 ($\pm4\%$)	-3141 ($\pm4\%$)	-10%
Sea salt	-2494 ($\pm2\%$)	-1477 ($\pm1\%$)	-41%	-19 ($\pm2\%$)	-33 ($\pm2\%$)	$+76\%$	-2513 ($\pm2\%$)	-1510 ($\pm1\%$)	-40%
MOA	-7.59 ($\pm2\%$)	-4.45 ($\pm1\%$)	-41%	-0.36 ($\pm2\%$)	-0.42 ($\pm3\%$)	$+16\%$	-7.94 ($\pm2\%$)	-4.87 ($\pm1\%$)	-39%
BC	-3.26 ($\pm8\%$)	-2.57 ($\pm7\%$)	-21%	-0.00 ($\pm14\%$)	-0.00 ($\pm19\%$)	$+22\%$	-3.26 ($\pm8\%$)	-2.58 ($\pm7\%$)	-21%
POA	-15.18 ($\pm7\%$)	-12.86 ($\pm7\%$)	-15%	-0.01 ($\pm29\%$)	-0.02 ($\pm41\%$)	$+15\%$	-15.19 ($\pm7\%$)	-12.88 ($\pm7\%$)	-15%